

## Dimension Measurements for Geostrophic Turbulence

John Guckenheimer

*Division of Natural Sciences, University of California, Santa Cruz, California 95064*

and

George Buzyna

*Geophysical Fluid Dynamics Institute, Florida State University, Tallahassee, Florida 32306*

(Received 20 July 1983)

The transition to geostrophic turbulence in a rotating annulus experiment has characteristics which differ from the scenarios for the transition to turbulence which have been previously described. Estimates of dimension from the experimental data suggest a mechanism in which a discrete symmetry of the preturbulent state plays an important role. The techniques used for the dimension estimates are new and substantially more efficient than those used previously.

PACS numbers: 47.25.Qv, 47.10.+g

A rotating, differentially heated annulus of fluid is a classical laboratory model for the large-scale midlatitude circulation of the Earth's atmosphere.<sup>1</sup> Extensive investigation has classified large portions of the stability diagram for these laboratory systems in a parameter plane representing Rossby and Taylor numbers.<sup>2,3</sup> Figure 1 illustrates the behavior from one set of experiments conducted at the Geophysical Fluid Dynamics Institute, and described in detail elsewhere.<sup>4</sup> This Letter reports the results of additional analysis of the data from these experiments, analysis directed towards characterizing the transition to geostrophic turbulence.

Experiments with Rayleigh-Bénard convection<sup>5</sup> have revealed substantial qualitative differences in the transition to aperiodic flow in small- and large-aspect-ratio containers. With small-aspect-ratio containers, there is a close parallel between the routes to chaos found in nonlinear dynamical systems with a low-dimensional state space and the transitions observed experimentally.<sup>6</sup> We were motivated to examine the transition to geostrophic turbulence in a rotating annulus because the experimental data did not appear consistent with the mechanisms by which a quasi-periodic motion becomes aperiodic in simulations of low-dimensional systems.<sup>7</sup> Our analysis confirms this conclusion, but we discuss our methods before presenting these results and speculating on their significance.

Previous efforts to calculate the dimension of attractors<sup>8</sup> have required significant amounts of computation. The methods employed here are much more efficient though they seem subject to larger statistical fluctuations when applied to a given amount of data. The theory underlying the method will be developed in more detail else-

where, but we give a brief sketch here. Strange attractors are complicated geometric objects, typically with a fractal structure,<sup>9</sup> which appear in the state space of chaotic flows. The problem which confronts us is the specification of a reasonable definition of the dimension of an attractor

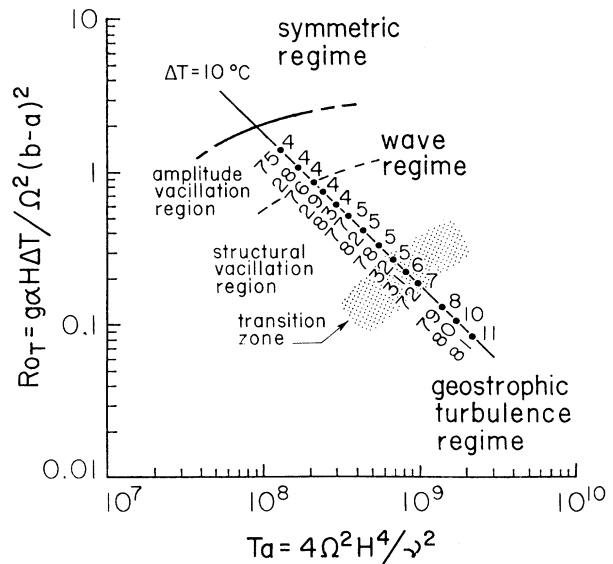


FIG. 1. Regime diagram, Rossby number ( $Ro_T$ ) vs Taylor number ( $Ta$ ) for experimental series C, showing the relative location in parameter space of different time-dependent behaviors. Dots along the diagonal line correspond to a sequence of experiments at a constant imposed temperature contrast  $\Delta T$  and at successively higher rotation rates  $\Omega$  ( $\Omega$  is lowest for experiment 75 and increases in the direction of experiment 81; experiment number is indicated to the left of each dot). The number shown to the right of each dot represents the dominant azimuthal wave number in the wave regime, and the peak of the broad wave-number spectrum in the geostrophic turbulence regime.

which can be readily estimated. Intuitively, the dimension should roughly correspond to the number of independent measurements which must be made to distinguish distinct states of the fluid *on the attractor*. In these measurements of dimension, we weigh regions of the attractor by the frequency with which a typical trajectory visits them through the introduction of an invariant measure  $\mu$  supported on the attractor.

Our strategy for computing dimension is adapted from the work of Billingsley<sup>10</sup> and Young.<sup>11</sup> Let  $\mu$  be a measure on  $R^n$  and  $\Lambda$  be a set of positive  $\mu$  measure. Denote the ball of radius  $r$  centered at  $x$  by  $B_x(r)$  and its  $\mu$  volume by  $V_x(r) = \mu(B_x(r))$ . Young<sup>11</sup> proves that if for  $x \in \Lambda$ ,

$$\underline{\delta} \leq \liminf_{r \rightarrow 0} \frac{\ln V_x(r)}{\ln r} \leq \limsup_{r \rightarrow 0} \frac{\ln V_x(r)}{\ln r} \leq \bar{\delta},$$

then the Hausdorff dimension of  $\Lambda$ ,  $D_H(\Lambda)$ , satisfies

$$\underline{\delta} \leq D_H(\Lambda) \leq \bar{\delta}.$$

We adapt this technique for dimension calculations by *assuming* that for almost all points  $x$  of the attractor (relative to  $\mu$ ), the limits in the above inequalities exist and are independent of  $x$ . An estimate for the dimension of the attractor is then given by calculating the function  $V_x(r)$  for a typical point  $x$  and plotting  $\ln V_x(r)$  vs  $\ln r$ . The calculation of  $V_x(r)$  proceeds by *assuming* that an experimentally observed trajectory gives a good random sample of points on the attractor relative to the measure  $\mu$ . For attractors whose dimension is not very small, this assumption is nontrivial because very long trajectories are needed to sample all regions of the attractors. We return to this point in later discussion. Our dimension estimates accept the estimate that  $V_x(r)$  is the proportion of points in the observed trajectory which lie within distance  $r$  of the point  $x$ .

The calculations themselves proceed efficiently, as follows. One begins with an experimentally observed trajectory of  $N+1$  points which is assumed to be on an attractor and lack transient behavior. From this trajectory, one selects a reference point  $x$  and computes the distance  $d_i$  from  $x$  to the other  $N$  points  $y_i$  of the trajectory. The list of distances  $d_i$  are then sorted numerically. From the sorted list, one reads that the  $i$ th largest distance gives a value of  $r$  for which  $V_x(r) = i/N$ . We have plotted these values for  $i = 2^j$  ( $j=1, \dots, k$ ;  $j = \log_2 N$ ) on a log-log plot of  $r$  vs  $V_x(r)$ . The dimension is estimated from such

a plot as the inverse of the slope of this curve. We caution, however, that the function  $V_x(r)$  need not be a smooth curve, so that an accurate estimation of the dimension may require a much wider range of values of  $r$  than one can hope to obtain experimentally or numerically.

To check the suitability of this strategy for calculating dimension, we performed several numerical tests. The results of one are shown in Fig. 2, where we display the log-log plots for seven separate collections of 5000 points on tori  $T^n$  of dimensions  $n=2, 3, 5, 10, 25, 50$ , and  $99$ . The straight lines in these plots have slopes which correspond to the different values of  $n$ . These experiments give us confidence that this method of calculating dimension gives good rough estimates with amounts of data that are readily obtainable from experiments and require only modest amounts of computation, on the order of  $N(\ln N + n)$  operations for  $N$  observations of  $n$ -variate data.

We have also tested the method on several modes of chaotic attractors, including the Hénon map,<sup>12</sup> the Lorenz equations,<sup>13</sup> and a map with an attracting nowhere differentiable torus.<sup>14</sup> These tests give results consistent with estimates obtained with use of other methods.<sup>8,15</sup> However, as noted by Pfeffer,<sup>16</sup> the method must be used with great caution and does not always give reli-

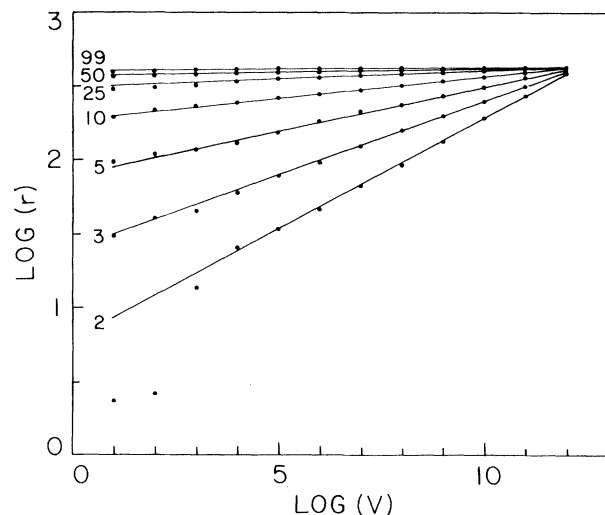


FIG. 2. Log-log plots of  $r$  vs  $V(r)$  for several numerical examples on tori  $T^n$  of dimension  $n=2, 3, 5, 10, 25, 50$ , and  $99$ . [Numerical values of  $\ln(r)$  represent a relative scale; numerical values shown on the  $\ln V$  axis represent  $j$  of the  $i=2^j$  value from the sorted list of data; see text.] The inverse of the slope is proportional to the dimension.

able results for reasonable models of some of the experiments analyzed here (cf. the discussion of amplitude vacillation below.)

Let us return now to the experimental data. The results of our dimension computation are displayed in Fig. 3. The apparatus contained 2016 thermistors in an annulus with inner and outer radii  $30.48 \pm 0.01$  and  $60.96 \pm 0.01$  cm. The working fluid, 1.52-cS ( $1 \text{ S} = 1 \text{ cm}^2/\text{sec}$ ) silicone fluid (Prandtl number  $N_{Pr} = 21$ ), had a free top surface and a depth of 15.00 to 0.05 cm. To perform our computations, we selected recordings from 27 thermistors located near middepth and well away from the walls of the rotating annulus. The number 27 was arbitrarily chosen to be large enough to represent the dimensions of the attractors we expected to find. The "distance"  $d_t$  represents here a maximum absolute value of the 27 temperature differences between the reference point  $x$

and another point  $y_t$  of the trajectory. Dimension calculations based upon a larger number of thermistors are in progress.

The stability diagram of Fig. 1 shows four distinct regimes, three of which represent time-dependent flows. In the region of amplitude vacillation, the fluid motion is quasiperiodic. If one models this quasiperiodic motion as a superposition of traveling waves, then Fourier analysis indicates that some 95% of the variance of the data is contained in four Fourier modes. Pfeffer<sup>16</sup> observed that our dimension estimates underestimate the dimension corresponding to a superposition of  $n$ -linear traveling waves, and we can show that the method yields a dimension estimate of  $\frac{1}{2}(n+1)$  if the temporal frequencies of the waves are independent. For the experimental data, our dimension estimates are consistent with a model represented by the superposition of four traveling waves. The data are insufficient to determine whether there are two, three, or four independent frequencies.

The dynamics of the structural vacillation regime are still not fully characterized. The estimated dimension of 1.6 for the structural vacillation regime is surprisingly small and requires further investigation. The dimension measurements shown in Fig. 3 indicate that, as the rotation rate of the apparatus increases, there is a jump in the dimension of the attractor which begins at small amplitude in phase space and grows continuously. As the amplitude of this high-dimensional motion approaches the amplitude of the dominant wave itself, the fluid undergoes the transition to geostrophic turbulence. Conservative estimates for the dimension of the attractor in these regimes are within the range of 7 to 12.

The jump in dimension from the amplitude vacillation regime through the structural vacillation regime is a departure from the scenarios for the transition to chaos which have been described for low-dimensional dynamical systems that deserves explanation. There is a dynamical mechanism which appears consistent with our measurements and other information about this flow. The observed flow in the structural vacillation regime has an (approximate) discrete spatial symmetry which corresponds to rotation by  $2\pi/4$  or  $2\pi/5$  in the experiments analyzed in the structural vacillation regime. If a new asymmetric oscillatory mode of instability appears in the fluid motion, then the symmetry of the fluid equations and the motion prior to the instability force the instability to be degenerate. The translates of the asym-

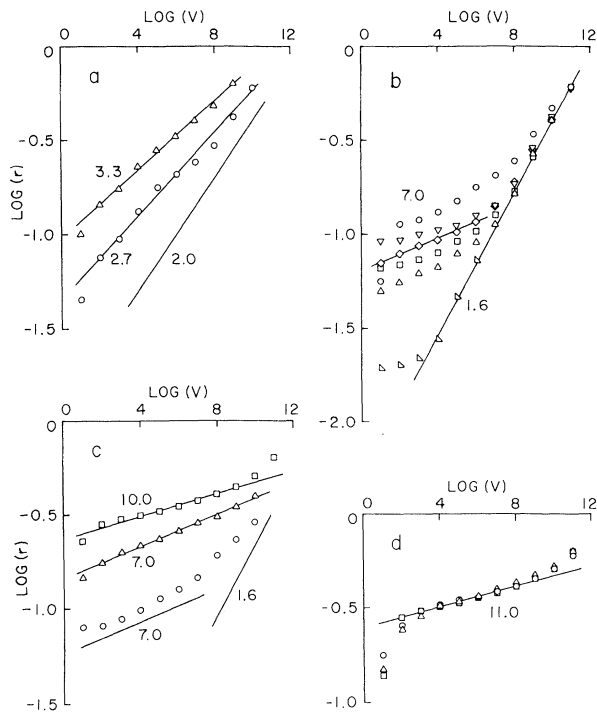


FIG. 3. Log-log plots of  $r$  vs  $V(r)$  for the experimental series (coordinate axes scaled as in Fig. 2). (a) Amplitude vacillation region; symbols and experiment numbers in order of increasing rotation rate are, respectively, circles, 75; and triangles, 28. (b) Structural vacillation region: right triangles, 76; triangles, 29; squares, 83; inverse triangles, 77; diamonds, 82; and circles, 78. (c) Transition zone: circles, 32; triangles, 31; and squares, 72. (d) Geostrophic turbulence regime; circles, 79; triangles, 80; and squares, 81.

metric oscillatory mode by the symmetry group would be distinct oscillatory modes. Thus, it is plausible that a quasiperiodic state with fivefold symmetry would evolve into an attractor with a jump in dimension from 2 to 7.

An alternative hypothesis to the scenario described above is that random effects or noise are responsible for the growing disorder of the fluid in the structural vacillation regime. Guckenheimer<sup>17</sup> presents methods for distinguishing the effects of noise and deterministic chaos upon experimental data by analyzing the short-term evolution of nearby initial states. These methods do not seem to be practical here because the dimension of the attractors is too large. Recalling our assumption in the dimension computations that the trajectory represented by the experimental observations was randomly distributed on the attractor, one can estimate the expected recurrence time for a trajectory. This recurrence time grows exponentially with dimension and is experimentally unreasonable for attractors of even moderate dimension. Detailed reconstructions of the dynamics of attractors from experimental data are feasible only for attractors of low dimension. Geostrophic turbulence does not appear to be a fluid state represented by a low-dimensional attractor, suggesting that further understanding of this fluid state will require a statistical methodology.

We wish to thank R. L. Pfeffer for his support and encouragement. One of us (J.G.) would also like to thank Uriel Frisch for conversations which prompted the development of the methods used here. This research was supported in part

by the U. S. Office of Naval Research (Contract No. N00014-77-C-0265), the U. S. Air Force Office of Scientific Research (Contract No. 83-0143), and the National Science Foundation (Grant No. MCS92-002260).

<sup>1</sup>D. Fultz *et al.*, Meteorol. Monogr. No. 21, 96, 97 (1959).

<sup>2</sup>R. Hide and P. J. Mason, Adv. Phys. 24, 47-100 (1975).

<sup>3</sup>R. L. Pfeffer, G. Buzyna, and R. Kung, J. Atmos. Sci. 37, 2129-2149, 2577-2599 (1980).

<sup>4</sup>G. Buzyna, R. L. Pfeffer, and R. Kung, to be published.

<sup>5</sup>G. Ahlers and R. P. Behringer, Phys. Rev. Lett. 40, 712-716 (1978).

<sup>6</sup>J. P. Gollub and S. V. Benson, J. Fluid Mech. 100, 449-470 (1980).

<sup>7</sup>J. P. Eckmann, Rev. Mod. Phys. 53, 643-654 (1981).

<sup>8</sup>D. Russel, J. Hansen, and E. Ott, Phys. Rev. Lett. 45, 1175 (1980).

<sup>9</sup>B. Mandelbrot, *The Fractal Geometry of Nature* (Freeman, San Francisco, 1982).

<sup>10</sup>P. Billingsley, *Ergodic Theory and Information* (Wiley, New York, 1965).

<sup>11</sup>L.-S. Young, "Dimension, Entropy and Lyapunov Exponents" (to be published).

<sup>12</sup>M. Hénon, Commun. Math. Phys. 50, 69 (1976).

<sup>13</sup>E. Lorenz, J. Atmos. Sci. 20, 130 (1963).

<sup>14</sup>J. D. Farmer, E. Ott, and J. Yorke, to be published.

<sup>15</sup>P. Grassberger and I. Procaccia, Phys. Rev. Lett. 50, 346 (1983).

<sup>16</sup>R. Pfeffer, private communication.

<sup>17</sup>J. Guckenheimer, Nature (London) 298, 358-361 (1982).